



## Alginate/CaCO<sub>3</sub> hybrid Loaded with Sorafenibtosylate and Gold Hexagons: A Model for Efficient Dual (Chemo-Radio) Treatment of HepG2

Firas A. Sukkar,<sup>a</sup> Medhat W. Shafaa,<sup>a</sup> Mohamed S. El-Nagdy,<sup>a</sup> Wael M. Darwish,<sup>b\*</sup>



CrossMark

<sup>a</sup> Physics Department, Faculty of Science, Helwan University, Cairo, Egypt

<sup>b</sup> Department of Polymers and Pigments, National Research Centre, Elbohouth Street, Dokki12622 Giza, Egypt

### Abstract

We investigated the combinatorial cytotoxic actions of the chemotherapeutic drug (sorafenib tosylate, ST), in synergism with  $\gamma$ -radiation, on human hepatocellular carcinoma (HepG2) cells. The novel radiosensitizer, hexagonal gold nanoparticles (HG), was prepared and utilized to enhance the radiobiological response of HepG2 cells. A well-designed nanoporous alginate/calcium carbonate hybrid (ALG-CaCO<sub>3</sub>) was prepared as a biocompatible/biodegradable nanocarrier for co-delivery of the hydrophobic drug (ST) and the hydrophilic radiosensitizer (HG) to the cancer cells. Incubation of HepG2 cells with the prepared nanopores followed by irradiation with different doses (0, 3 or 6 Gy) of  $\gamma$ -radiation resulted in a significant reduction of the cells viability as a result of the synergistic (chemo-radiation) cytotoxic actions.

*Keywords:* Alginate; hexagonal gold; sorafenib; HepG2; radiotherapy

### 1. Introduction

Nanotechnology provides several methods for physical encapsulation of hydrophilic and/or hydrophobic drugs in biocompatible polymers in mild conditions [1]. Nanocapsules made of natural polymers such as alginates and chitosan can enhance the biocompatibility and blood pharmacokinetics of the loaded drug, while reduce its side effects [2,3]. Polymeric nanoparticles, especially those made of natural polymers such as alginates, are promising platforms for formulating combination cancer therapeutic models [4]. A special interest in the pharmaceutical industry has been given to alginates because of its excellent biodegradability, biocompatibility, nontoxicity, chelating ability, and relatively low cost. Alginates are anionic hydrophilic polysaccharide mostly used for production of biocompatible/biodegradable delivery systems for cancer drugs. Alginate nanoparticles are usually obtained by inducing the crosslinking of an alginate

solution with calcium chloride. When sodium alginate solution is added into a solution of calcium ions, the calcium ions displace the sodium ions in the alginate polymer [5]. Alginate is a biosynthesized natural polymer derived from two main sources: marine plants and bacteria [6]. The chemical and physiological properties of alginates have been intensively studied [7]. The chemical structure of alginate polymer allows for several modifications with an excellent impact on their drug release behavior compared with unmodified alginate. For instance, alginates that are rich in l-gulonate form strong but brittle gels, whereas alginates rich in d-mannuronate are more flexible [8]. Sorafenib tosylate (ST) a tyrosine kinase antagonist is one of the most efficient antineoplastic for treatment of advanced hepatocellular carcinoma [9]. However, the low bioavailability, hepatic first path and cell resistivity are the main challenges towards achieving high potency of ST in the clinical therapy [10]. To address such issues, many approaches have been

\*Corresponding author e-mail: [wmdarwish55@gmail.com](mailto:wmdarwish55@gmail.com); (Wael M. Darwish).

Received: 04 September 2021; Revised: 29 September 2021; Accept: 08 November 2021

DOI: [10.21608/EJCHEM.2021.94234.4434](https://doi.org/10.21608/EJCHEM.2021.94234.4434)

©2022 National Information and Documentation Center (NIDOC)

developed such as incorporation of ST in nanoparticles made of biodegradable polymers [11,12]. In the other side, radiation therapy has been one of the most potent modalities for treatment of malignant solid tumors [13]. The major challenge towards optimized potency of radiation therapy is focusing the radiation dose to the malignant tissues with minimal damage to the normal tissues in the surrounds [14,15]. One way to elevate the radiobiological response of the cancer cells is the use of radiosensitizers. Radiosensitization effect arises from interaction of ionizing radiation with high-Z (atomic number) materials resulting in enhancement of Auger electron emission [16]. The low energy and short effective zone of Auger electrons lead to deposition of energy around the nanoparticles localized at the tumor sites [17]. Radiosensitizers, such as gold nanoparticles, improve the response of hypoxic tumor cells to the ionizing radiation even at low radiation doses [18]. This is mainly attributed to their strong photoelectric absorption coefficient [19]. Gold nanoshapes are biocompatible, apparently non-toxic and mainly cleared from the body through the kidneys [20]. Chemotherapy is usually recommended as an adjuvant treatment in combination with radiotherapy [21,22]. However, synergistic cytotoxic effects of the combined therapeutics are essential when a dual treatment model is designed [23]. Tailor-made polymeric nanoparticles are advantageous platforms for production of synergetic dual modalities. In this work, we investigated combination of the chemotherapeutic drug (sorafenib tosylate, ST) in synergism with gold-sensitized  $\gamma$ -radiation therapy. In this study, nanoporous alginate/CaCO<sub>3</sub> hybrid was proposed as a nanocarrier aiming to enhance the bioavailability and release profile of the hydrophobic ST. Additionally, nanoporous alginate/CaCO<sub>3</sub> hybrid has hydrophilic sites where the hydrophilic novel radiosensitizer (gold hexagonal nanoparticles) can be co-encapsulated. The proposed combinatorial model (HG-ST-ALG in synergism with  $\gamma$ -radiation) is promising for effective and minimally invasive treatment of HepG2 cells.

## 2. Materials and Methods

### 2.1. Materials

Sodium alginate was a product of PanReac AppliChem, Italy. Chloroauric acid (HAuCl<sub>4</sub>.4H<sub>2</sub>O, 99.99%), chitosan (CAS 9012-76-4) low viscosity

from shrimp shells, and sorafenib tosylate, ST (99%) were products of Sigma (Merck), Germany. Chitosan (CS) was refined by dissolving in 0.1% acetic acid followed by filtration and reprecipitation by dropping of 20N aqueous sodium hydroxide [24]. D-(+)-Glucono-1,5-lactone was a product of Alfa Aesar (CAS 90-80-2). Other reagents and solvents were of analytical grade. Milli-Q water was used for the preparation of the final formulations, otherwise deionized water was used. Sterilized dialysis tubing with molecular weight cut-off (MWCO 3kDa) was purchased from Cellulose Dialysis Tubing, Fisherbrand, USA. All glassware and magnetic stir bars used in the syntheses were thoroughly cleaned in aqua regia rinsed in distilled water, and then oven-dried prior to use.

### 2.2. Methods

Transmission electron microscope (TEM) images were recorded on a JEM-2100, Jeol electron microscope. The hydrodynamic mean diameter and size distribution of the prepared gold and polymeric nanoparticles were determined, after samples dilution, by Dynamic Light Scattering (DLS) instrument (PSS, Santa Barbara, CA, USA), using the 632 nm line of a He-Ne laser as the incident light with angle 90° and zeta potential with external angle 18.9°. Optical extinction spectra were recorded at room temperature using a computerized Cary 300 spectrophotometer, Agilent Technologies, over a spectral range between 400 and 1000 nm and a spectral resolution of 2 nm. Differential scanning calorimetric (DSC) analysis were carried out on DSC131 evo (SETARAM Inc., France), Central Laboratories Network, National Research Centre (NRC), Egypt. The instrument was calibrated using the standards (Mercury, Indium, Tin, Lead, Zinc and Aluminum). The test was programmed including the heating zone from 25°C to 400°C with a heating rate 10 °C / min. The samples were weighed in aluminum crucible 120  $\mu$ L and introduced to the DSC. The thermogram results were processed using (CALISTO Data processing software v.149). Gold analysis was carried out using a double beam flame atomic absorption, Agilent 240FS equipped with cross flow nebulizer.

### 2.3. Preparation of hexagonal gold nanoparticles (HG)

A solution of 1% concentration of D-(+)-Glucono-1,5-lactone was prepared by dissolving in Milli-Q

ultrapure water 18.2 MΩ.cm at 25 °C. Chitosan was dissolved in lactone solution to give a final chitosan concentration of (0.05%, w/v). After passage through 0.22 μm pore size filter membrane, the chitosan solution was brought to boiling. Aqueous solution of H<sub>2</sub>AuCl<sub>4</sub>.3H<sub>2</sub>O (200 μL, 49 mg/ml) was added to the boiling solution. The ruby red color characteristic for gold nanoparticles was observed after 10 minutes. After cooling to room temperature, gold hexagonal nanoparticles were separated by centrifugation (13,000 rpm, 4°C). Purification was carried out thrice by sonication in pure water followed by centrifugation. The solid was redispersed in ultrapure water and stored in dark at 4 °C till characterization. The characteristic plasmonic peak of HG colloid at λ<sub>max</sub> = 536 nm showed no shift or broadening after storage at these conditions for one month. This stability is mainly attributed to lactone and chitosan coats on the surface of the particles.

#### 2.4. Preparation of alginate nanoparticles

In this work, we provide a facile method for synthesis of gold hexagonal nanoparticles (HG). Firstly, sodium alginate was purified by dissolving in DW, passage through a filter (0.45 μm) and finally dropping acetone till a white precipitate is formed [25]. The solid was dried at room temperature under reduced pressure. Accurately weighed 60 mg of the purified alginate was dissolved in 10 ml of DW at 30 °C. Afterwards, 7 ml of aqueous calcium chloride solution (0.02 M) was added and the mixture was stirred for 30 min. A previously prepared aqueous solution of sodium carbonate (7 ml, 0.02 M) was then added followed by stirring for 3 h. The solid was separated by centrifugation (3500 rpm, 10 min). The white solid was washed twice with DW. The microparticles suspension was freeze-dried and the lyophilized powder was stored at 4 °C for characterization. For drug loading, acetone solution of ST (2 mg in 2 ml) was added to 10 mg of the lyophilized alginate powder and the mixture was stirred for 12 h to evaporate the organic solvent. The solid was washed with 20% aqueous solution of tween 20 before washing twice with DW. Finally, the colloid was subjected to freeze-drying and stored in dark at 4 °C. For loading of HG, acetone solution of lyophilized HG (100 μg in 1 ml) was added followed by the same procedure for separation and purification. For loading of both ST and HG, acetone solution containing 2 mg of ST and 100 μg of HG was used. Preliminary studies were carried out to

assess the optimized conditions (concentrations and temperature) aiming at preparation of monodispersed nanoparticles featured with high drug payload.

#### 2.5. Estimation of drug content and encapsulation efficiency

During the synthesis procedures of the gold and/or ST containing alginate nanoparticles, acetone supernatants were collected and analyzed for the unloaded (free) amounts of HG and/or ST. Thus, the loaded amounts of HG and ST can be calculated by abstracting the unloaded amounts from the total added amounts of each species. Concentration of gold in the supernatant was determined using atomic absorption spectroscopy as previously describe [18]. Concentration of ST was determined via spectroscopic method by monitoring the characteristic absorption of sorafenib tosylate in organic solvents at 264 nm [26]. Drug loading (mg/g) and percent encapsulation efficiency (% EE) were calculated according to equations 1-2, where (C<sub>s</sub>) is the concentration of HG or ST in the supernatant and the total concentration of each species (C<sub>t</sub>).

Drug Loading (mg/g) =  $(C_t - C_s) / (\text{Weight of the NPs powder})$  [1]

Encapsulation Efficiency (%) =  $(C_t - C_s) / C_t \times 100$  [2]

#### 2.6. In-vitro release profile of ST

The release profiles of sorafenib tosylate (ST) from the nanoparticles were studied as follows: 10 mg of the lyophilized powder was dispersed in 4 ml of PBS (pH 7.4) and put in dialysis tubing (MWCO 3 KDa). The bag was immersed in 20 ml of dialysate (phosphate-buffered saline, PBS, pH 7.4) under air bath thermostat (37 ± 0.5 °C, 180 rpm). At successive time intervals (1 - 72 h), exactly 1 ml of the dialysate was taken out and replaced with 1 ml of fresh PBS. The dialysate aliquots were analyzed for ST concentration by monitoring the decrease in the absorption of sorafenib tosylate in aqueous medium at 265 nm, as previously described [27]. For determining the released amount of HG, the dialysate was analyzed for gold concentration by digestion in preheated nitric acid followed by atomic absorption method. The same experiments were repeated while the dialysate solution is (phosphate-buffered saline, PBS, pH 5.2).

### 2.7. Cell viability assay

Liver cancer cells (HepG2) were obtained from American Type Culture Collection and were cultured at 37°C in RPMI-1640 medium supplemented with 10% fetal bovine serum (FBS), L-glutamine (200 mM), penicillin (100 U/ml), streptomycin (100 µg/ml), and HEPES buffer (1M) (All from Biowest, Nuaille, France). When reaching confluence, monolayer cells were rinsed with phosphate buffered saline (PBS) and harvested by trypsin/EDTA (Biowest) treatment. After treatment of cells with the formulations containing different concentration of HG and ST and incubation for 48 h at 37°C, the plates were examined under the inverted microscope and proceeded for the MTT assay [28].

### 2.8. Cells irradiation

After incubation of the cells with different formulations for 48 h, the media was replaced with fresh media and the cells were irradiated with different radiation doses (3 and 6 Gy) by cesium-137 source and incubated at 37 °C for 24 h. The source-to-cell surfaces distance was adjusted at 100 cm for the irradiated culture plates at a radiation field size of 15×15 cm<sup>2</sup>. Twenty four hours post irradiation, cell viability was assessed by incubating the cells for 2 h with a medium containing neutral red solution. After replacing the media several times, the dye in each well was extracted and the absorbance at a wavelength of 570 nm was read using a plate reader (Victor 3V-1420, Finland). Sensitization enhancement ratio (SERs) of various treatment groups was calculated and compared using HepG2 cells. (SERs) were calculated by dividing the surviving fraction of the irradiated cells in the absence of gold on the surviving fraction in presence of gold for each dose of radiation according to standard protocols [29].

### 2.9. Statistical analysis

All experiments were repeated three times (n = 3) and differences in the data were evaluated with one way ANOVA test. The data are given as a mean ± standard deviation (SD) at statistically significant values (P < 0.05).

## 3. Results and Discussion

In this work, we investigated the synergistic cytotoxic actions of the chemotherapeutic (ST), combined with gold-sensitized  $\gamma$ -radiation, on human

hepatocellular carcinoma (HepG2) cells. For this purpose, hexagonal gold nanoparticles were prepared and used as a novel radiosensitizer to enhance the radiobiological response of HepG2 cells. Nanoporous alginate/CaCO<sub>3</sub> hybrid was prepared as a biocompatible/biodegradable nanocarrier for physical encapsulation of the hydrophilic hexagonal gold nanoparticles (HG) and the hydrophobic drug (ST). The proposed combination regimen was designed to target key pathways in a characteristically synergistic or an additive manner.

### 3.1. Hexagonal gold nanoparticles

Size, shape and coating of the gold nanoparticles determine their ability of cellular internalization and radiosensitization efficacy [18,30]. In the present study, a facile procedure for synthesis of gold hexagonal nanocrystals (HG) is described. The radiosensitization effect of HG was used. Chitosan was used to reduce Au<sup>3+</sup> ions to atomic gold, where D-(+)-glucono-1,5-lactone was used to dissolve chitosan polymer instead of acetic acid. This led to formation of lactone-capped hexagonal nanocrystals (HG). The ruby-red color of colloidal gold (Fig. 1A) is characteristic for the excitation of surface plasmonic resonance of HG. Extinction spectra of aqueous lactone-capped HG colloid showed an extinction spectrum at 536 nm (Figs. 1B,C). Low magnification TEM images (Fig. 1B) showed hexagonal gold nanocrystals of average diameter of about 28 nm, while high magnification TEM images of HG (Fig. 1C) showed high degree of crystallinity. As predicted from dynamic light scattering (DLS) measurements, the particles have a mean hydrodynamic radius of 34.2±4.5 nm indicating the presence of thin layer coat of about 6 nm (Table 1). According to Zeta potential measurements, HG NPs have a negative surface charge of -14.62 mV (Table 1) and this suggests the lactone capping on the surface of the gold hexagons. We likely ascribe the formation of hexagonal nanocrystals to the relatively slow growth of gold crystals in the viscous lactone medium. Apparently, lactone capping instead of chitosan capping contribute to the formation of the hexagonal-shaped nanocrystals. Generally, the proposed surfactant-free procedure for preparation of HG is more favored than the surfactant-based method [31] and more facile than other previously described procedures [13,32].

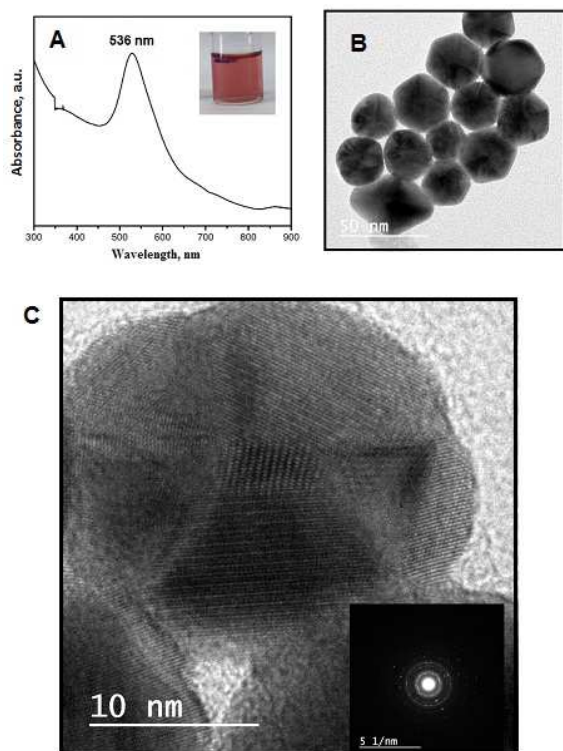


Fig. 1. Extinction spectra of aqueous HG colloid (A), TEM image of hexagonal gold nanoparticles (B), high magnification TEM images of HG (C), Inset, electron diffractogram of HG NPs.

### 3.2. Alginate/CaCO<sub>3</sub> polyelectrolyte nanoparticles

This study aims to investigate the cytotoxic actions of gold hexagons-sensitized radiation in synergism with sorafenib tosylate against human hepatoma HepG2 cells. The key parameter in such combinatorial model is the choice of a nanocarrier capable for incorporating and co-delivery of both the hydrophobic drug (sorafenib tosylate) and the hydrophilic radiosensitizer (hexagonal gold nanoparticles). Alginate has a linear polysaccharide structure comprising linear blocks of (1 → 4)-linked β-d-mannuronic acid (M) and α-l-guluronic acid (G) monomers [6-8]. This copolymer comprises three forms of polymer segments: consecutive G residues, consecutive M residues, and alternating MG residues (Fig 2). Therefore, alginate copolymer consists of different compositions, sequence, and variable molecular weights according to its source.

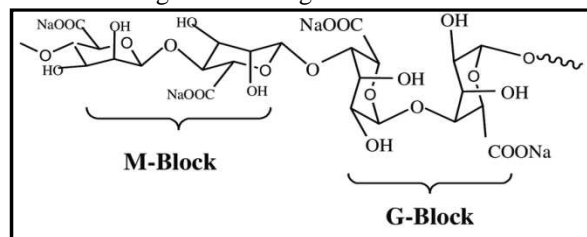


Fig. 2. Molecular structure of sodium alginate [8]

Alginate hybrid is capable for loading different therapeutics regardless of their surface charge and hydrophilicity [33, 34]. Nanoporous alginate/CaCO<sub>3</sub> hybrid platform is significant in that the hydrophilic anionic alginate sites can be loaded with the hydrophilic gold hexagons, while the nanosized porous can be loaded with the hydrophobic drug (ST). Divalent cations like Ca<sup>2+</sup> can induce interchain association with G units of the alginate polymer forming junction zones (Fig. 3). After addition of Na<sub>2</sub>CO<sub>3</sub>, carbonate anions tend to deprive the coordinated calcium cations as CaCO<sub>3</sub>, while the polymer chains prevent the precipitation of CaCO<sub>3</sub>. Thus, Ca<sup>2+</sup> rich sites will be condensed in the core of the nanoparticle with formation of nanosized pores, whereas Ca<sup>2+</sup> deficient sites will be enlarged in size due to repulsion between the anionic carboxylate groups (Fig. 3). In a previous work [35], the hydrophobic drug PTX was loaded in alginate hybrid followed by loading of the hydrophilic drug (DOX) and thus low amounts of DOX could be loaded because some nanoporous have been occupied by PTX. However, in this work, we aimed to achieve a simultaneous loading of the hydrophobic drug and the hydrophilic drug to avoid low loading of the hydrophilic drug in the previously described two steps loading process (Fig. 3)[35]. In this work, we proposed a one step procedure for production of the hydrophilic HG and the hydrophobic ST loaded alginate hybrid nanoparticles suitable as a combinatorial (chemo-radio) model for treatment of HepG2 cells. The physicochemical properties of the prepared nanoprobings were studied by TEM, DLS, Zeta-potential analyzer and DSC. TEM images (for example, Fig. 4) showed spherical nanoparticles with mean diameter of 230, 265, 290 and 295 nm for empty ALG, ST-ALG, HG-ALG and HG-ST-ALGNPs, respectively. The high magnification TEM image (Fig. 4 inset) shows porous structure of the prepared hybrid and hexagon-shaped gold nanoparticles.

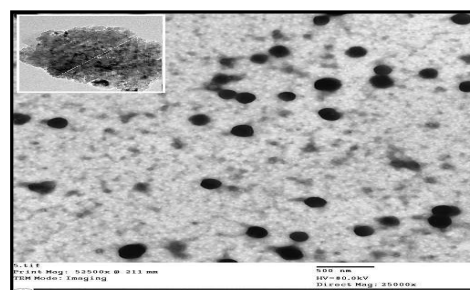


Fig. 4. TEM images of HG-ST-ALG NPs, sample was imaged after staining with phosphotungstic acid for better visualization of the polymeric nanoparticles. (inset: high magnification without staining)

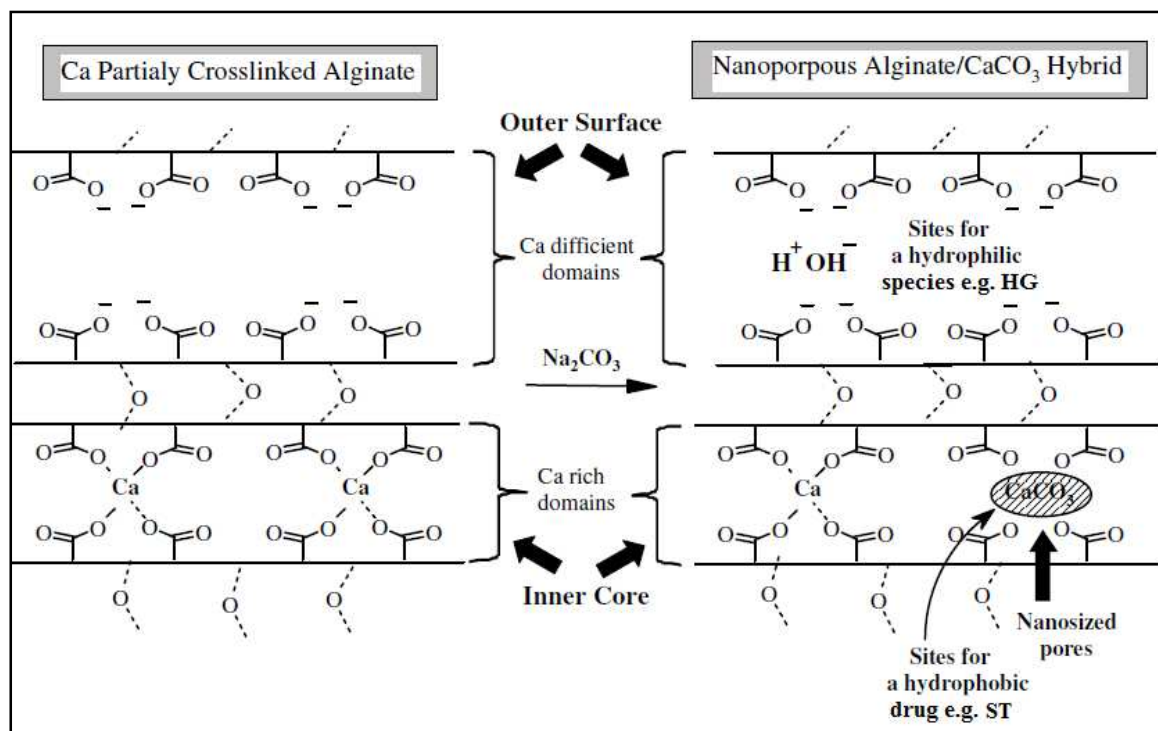


Fig. 3. Formation of nanoporous alginate/CaCO<sub>3</sub> hybrid with hydrophilic enlarged outer layer with water access suitable for loading of hydrophilic drug e.g. HG; and condensed calcium rich domains with calcium carbonate nanosized pores suitable for loading of a hydrophobic drug e.g. sorafenib (A diagram modified from reference 35).

Dynamic light scattering (DLS) measurements of the prepared polyelectrolyte nanoparticles showed average hydrodynamic diameters of  $345.4 \pm 4.2$ ,  $366.1 \pm 3.2$ ,  $390.9 \pm 2.9$  and  $405.8 \pm 6.2$  nm, for empty ALG, ST-ALG, HG-ALG and HG-ST-ALGNPs, respectively (Fig. 5). The hydrodynamic diameters of all prepared samples, measured by DLS of the aqueous colloid, are significantly higher than the mean diameter observed of the solid particles by TEM. This is mainly attributed to high diffusion of water to the outer hydrophilic layer of the hybrid. All nanoparticles showed a narrow size distribution (polydispersity index  $< 0.3$ ) and negative zeta potential (Table 1). The prepared nanoparticles are nearly monodispersed nanoparticles (PDI  $< 0.3$ ) (Fig. 5 and Table 1) and characterized with high drug loading and encapsulation efficiency (Tables 2). Nanoparticles are physically stable, due to the negative surface charges, and no significant changes in size, zeta potential, or drug content was observed for one month. Stability of the prepared nanoformulations was further proved by observing no changes in the extinction spectra of ST and HG in all formulations

before *in-vitro* studies. The amounts of ST and HG loaded in the nanoparticles were analyzed by a spectroscopic method and atomic absorption spectroscopy, respectively. Drug loading content and encapsulation efficiency of the prepared nanopores are compiled in Table 2. In the current work, the hydrophobic drug (ST) and the hydrophilic radiosensitizer (HG) were homogeneously dispersed in acetone and simultaneously loaded in hybrid alginate/CaCO<sub>3</sub>. Therefore, the loading amounts of ST in ST-ALG and HG-ST-ALG are comparable. In the other side, the hybrid alginate/CaCO<sub>3</sub> nanoparticles showed moderate loading capacity for both ST and HG. DSC measurements is an important tool in drug delivery systems to inspect the nature of the encapsulated drug (amorphous or crystalline) and the possible physicochemical interactions between the drug and the recipients used for design of the formulations [36, 37]. DSC measurements of pure ST (A), sodium alginate polymer (B), lyophilized empty ALG NPs (C) and HG-ST-ALG NPs (D) were carried out from room temperature to 400 °C (Fig. 6). The DSC thermogram of pure ST showed a sharp melting endotherm band at 241.2 °C (Fig. 6A) coincides with reported for sorafenib tosylate (240-243 °C)

indicating purity of the drug [36]. The DSC thermogram of sodium alginate polymer (Fig. 6B) showed an endothermic peak centered at 88°C and an exothermic peak centered at 256 °C corresponding to polymer dehydration and degradation, respectively [38]. The DSC thermogram of lyophilized empty ALG/CaCO<sub>3</sub> hybrid nanoparticles (Fig. 6C) exhibited a sharp endothermic band at 185 °C and a broad exothermic band from (260 °C to 295 °C). The endothermic band is probably assigned to cleavage enthalpies (breakage) of calcium-carboxylate bonds within the calcium rich sites of the complex forming the so called “egg-box” structure [38]. The broad exothermic band probably corresponds to degradation cross-linked alginate hybrid. The shift of this band to higher temperature, compared to that of alginate polymer, indicates that the cross-linked hybrid is more resistive to thermal degradation than the polymer. Lyophilized HG-ST-ALG NPs exhibited a DSC thermogram similar to that of empty ALG NPs (Fig. 6D), except the broadening of the endothermic peak, probably due to some lattice defects of alginate matrix due to inclusion of gold and sorafenib nanoparticles.

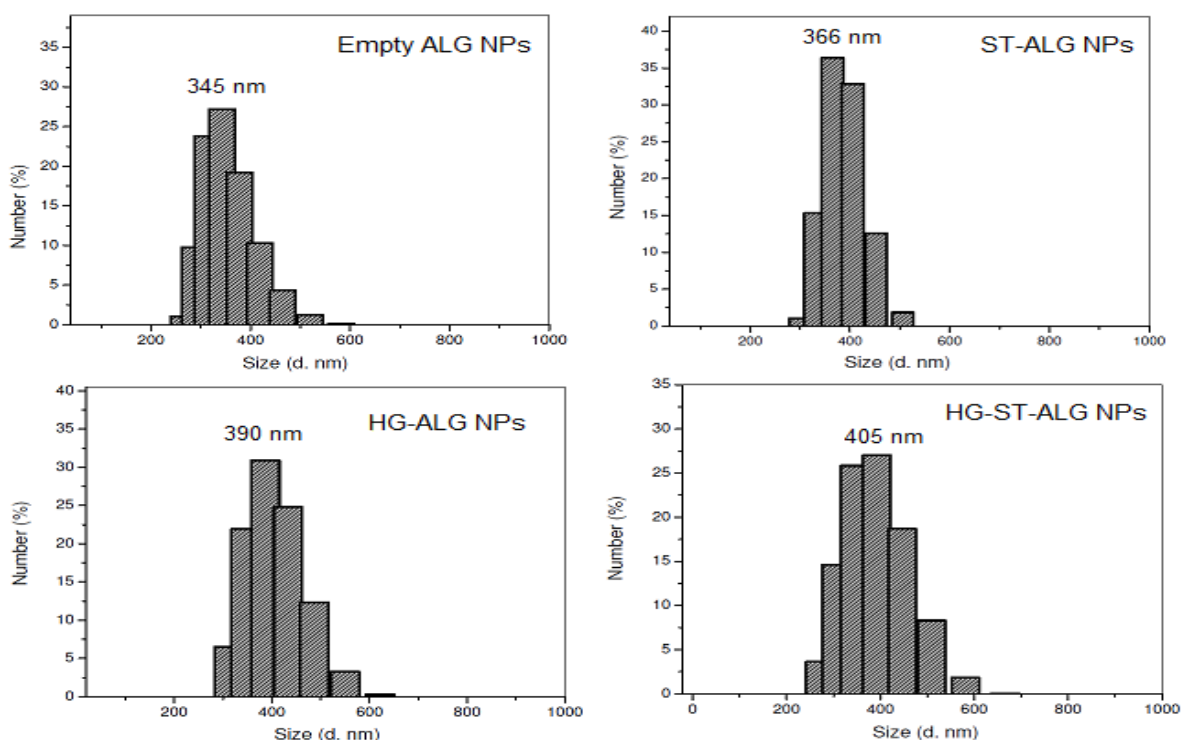


Fig. 5. Results of DLS measurements of the prepared nanoparticles

Table 1

Data of hydrodynamic diameters and zeta potential values of HG NPs, blank nanoparticles and drug loaded nanoparticles. The data correspond to the average of five independent batches and are presented as mean  $\pm$  SD

Formulation	$H_D \pm SD$ (nm)	PDI	$\zeta \pm SD$ (mV)
HG NPs	$34.2 \pm 4.5$	0.211	$-12.35 \pm 2.4$
Empty ALG NPs	$345.4 \pm 4.2$	0.205	$-20.1 \pm 1.9$
ST-ALG NPs	$366.1 \pm 3.2$	0.271	$-12.4 \pm 0.6$
HG-ST NPs	$390.9 \pm 2.9$	0.282	$-13.6 \pm 0.9$
HG-ST-ALG NPs	$405.8 \pm 6.2$	0.296	$-14.5 \pm 1.2$

Data of  $H_D$  and zeta potential represent the mean values  $\pm$  SD,  $n=3$ . Abbreviations ALG, a alginate/CaCO<sub>3</sub> hybrid nanoparticles, EE, encapsulation efficiency,  $H_D$ , the average hydrodynamic diameter estimated by DLS, HG, Hexagonal gold nanoparticles, PDI, polydispersity index, ST, sorafenib tosylate, SD, standard deviation,  $\zeta$ , zeta potential.

Table 2

Drug loading contents and encapsulation efficiencies of the drug loaded nanoparticles. The data correspond to the average of five independent batches and are presented as mean  $\pm$  SD

Formulation	DL (mg/g) $\pm$ SD		EE (%) $\pm$ SD	
	HG	ST	HG	ST
ST-ALG NPs	----	59 $\pm$ 3	----	42.6 $\pm$ 3.6
HG-ALG NPs	71 $\pm$ 4	----	58.4 $\pm$ 2.6	----
HG-ST-ALG NPs	64 $\pm$ 5	55 $\pm$ 4	47.8 $\pm$ 4.2	39.65 $\pm$ 3.7

Formulation	DL (mg/g) $\pm$ SD		EE (%) $\pm$ SD	
	HG	ST	HG	ST
ST-ALG NPs	----	59 $\pm$ 3	----	42.6 $\pm$ 3.6
HG-ALG NPs	71 $\pm$ 4	----	58.4 $\pm$ 2.6	----
HG-ST-ALG NPs	64 $\pm$ 5	55 $\pm$ 4	47.8 $\pm$ 4.2	39.65 $\pm$ 3.7

Note, Data represent the mean values  $\pm$  standard deviation (SD),  $n=3$ . Abbreviations ALG, alginate/ $\text{CaCO}_3$  hybrid nanoparticles, DL, drug loading, EE, encapsulation efficiency, HG, hexagonal gold nanoparticles, NPs, nanoparticles, ST, sorafenib tosylat.

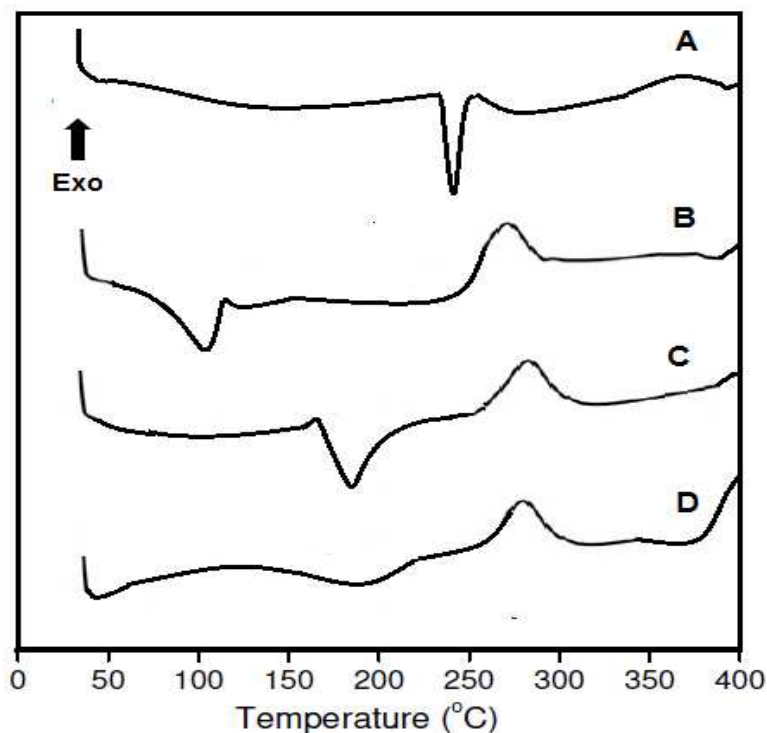


Fig. 6. DSC thermograms of ST (A), sodium alginate polymer (B), empty ALG/ $\text{CaCO}_3$  hybrid NPs (C), and HG-ST-ALG NPs (D).

### 3.3. *In-vitro* release study

Release profiles of ST revealed a sustained release from both ST-ALG and HG-ST-ALG nanoparticles within the first 72 hours (Fig. 7). For ST release in neutral media (pH 7.4), the driven mechanism of release is drug diffusion. Release of ST from both formulations in neutral media is slow and shows no burst release, probably due to the hydrophobicity of ST. A moderate release of ST is observed in acidic medium with optimum release of 62.1 % and 50.3 %, from ST-ALG and HG-ST-ALG nanoparticles, respectively (Fig. 7). A similar release profile was reported for release of the hydrophobic drug paclitaxel from alginate/ $\text{CaCO}_3$  hybrid



nanoparticles (ALG). Compared to release in neutral medium, the released amounts of ST are greater in acidic medium (pH5.2) from both ST containing formulations. This release behavior is adequate for cancer treatment due to the well-known acidic extracellular tumor environment [39,40]. It is well known that the acidic conditions accelerate the breaking down of particle structure and resulting in a fast diffusion of drug from the interior of the nanoparticles [41]. A steady and optimal release of ST was reached after 48 h.

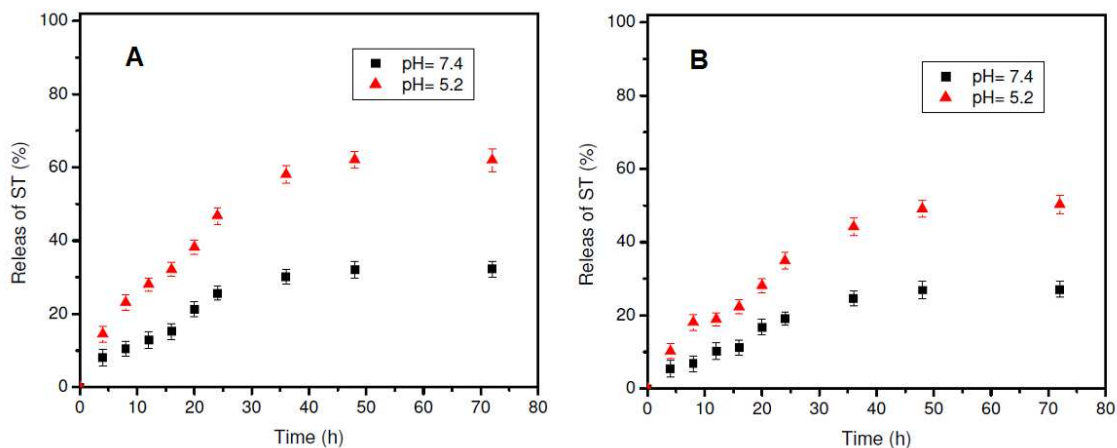


Fig. 7. *In-vitro* release profiles of ST from ST-ALG (A) and HG-ST-ALG (B) in neutral and acidic media.

### 3.4 *In-vitro* anticancer efficiency

In this work, the half-maximal inhibitory concentration ( $IC_{50}$ ) of sorafenib tosylate (ST) free drug on human hepatocarcinoma HepG2 cells of 18.9  $\mu\text{g/ml}$  was estimated from the dose response curve. This value is comparable to the previously reported value 17.5  $\mu\text{g/ml}$  [42]. Free drug samples were prepared by dissolving sorafenib in dimethyl sulfoxide (DMSO) and stored as stock solution at  $-20^{\circ}\text{C}$ .  $IC_{50}$  values of ST in ST-ALG and HG-ST-ALG were found to be 12.7 and 14.3  $\mu\text{g/ml}$ , respectively. It can be concluded that inclusion of ST in alginate nanoparticles significantly reduced the  $IC_{50}$  values of ST, compared to the free drug. This evidences the crucial role of the nanocarrier in the cellular internalization of the drug. To verify the cytotoxic effects of the proposed model on human hepatocarcinoma HepG2 cells, the cells were cultured and incubated with formulations containing different concentrations of sorafenib tosylate (0-24  $\mu\text{g/ml}$ ) followed by  $\gamma$ -irradiation with selected radiation doses (0, 3 and 6Gy) (Fig. 8A-C). According to gold analysis, the corresponding gold concentrations were found to be in the range of (0 - 25.2  $\mu\text{M}$ ). HepG2 cells were incubated with the formulations for 48 h before processing MTT assay (Fig. 8A-C). The cell viability results are summarized in the next two parts.

#### 3.4.1. Treatment without external radiation

Cell viabilities obtained after incubation of HepG2 cells with the prepared nanoprobe without subsequent external radiation represent the pure chemical cytotoxicity of the formulations (Fig. 8A). The results can be summarized as follows:

- Empty alginate nanoparticles (ALG) showed high biocompatibility to HepG2 cells with viability percentage more than 90%. Treatment of HepG2 cells with ST-ALG NPs showed a significant toxicity on HepG2 cells in a concentration dependent manner (Fig. 8A) and this evidences the efficient release and cellular internalization of ST nanoparticles. This is in accordance with the previous reports on the increment in cell cycle inhibition of cancer drugs when loaded in polymeric nanoparticles [43].
- HG-ALGNPs are nearly non-toxic to HepG2 cells and about 90% of the cells remain viable after treatment with the highest gold concentration. This is mainly ascribed to biocompatibility of HG nanoparticles at the tested concentrations (Fig. 8B). This may be attributed to elevated released amounts of HG from HG-ALG NPs.

HG-ST-ALG NPs are significantly toxic to HepG2 cells and this toxicity increases gradually with increasing the concentration of both ST and HG in the nanoparticles (Fig. 8C). It is noteworthy to mention that the synergistic effects of HG and ST are not observed in this set of experiments where no external radiation is applied. More than 40 % of HepG2 cells could survive even at the highest concentrations of both ST and HG.

### 3.4.2. Treatment with external radiation

To verify the cytotoxic effects of the combinatorial (chemo-radio) model, HepG2 cells were incubated with the prepared formulations at the same previously tested concentrations of HG and/or ST followed by  $\gamma$ -radiation (3 and 6 Gy) using Cs-137 source. The results of cell viability assay are illustrated in Figs. 8B,C. It can be concluded that:

- Incubation of HepG2 cells with empty ALG NPs followed by irradiation with 3 and 6 Gy showed moderate cytotoxicity and more than 60% of the cells remain viable. Since ALG NPs are nearly non-toxic to HepG2 cells in absence of external radiation (Fig. 8A), this cytotoxicity is mainly attributed to the radiobiological actions on HepG2 cells and generation of reactive oxygen species [20].
- Incubation of HepG2 cells with gold containing nanoparticles (HG-ALG or HG-ST-ALG) followed by  $\gamma$ -radiation (3 or 6 Gy) results in a significant reduction of the cell viability compared to irradiation without prior incubation with gold formulations. This effect increases with increasing of the concentration of the gold radiosensitizer. This evidences that gold hexagonal nanoparticles efficiently enhances the radiobiological response of HepG2 cells (Figs. 8B,C).
- Incubation of HepG2 cells with ST-ALG NPs followed by radiation doses of 3 or 6 Gy resulted in cytotoxicities higher than the corresponding values obtained for each individual treatment (Fig. 8). These results, together with the markedly increased cytotoxicity observed with increasing ST concentration, confirms the synergistic

cytotoxic actions of ST and the non-sensitized ionizing radiation on HepG2 cells.

- Incubation of HepG2 cells with gold-sensitized combined treatment model (HG-ST-ALG+ radiation doses of 3 or 6 Gy) resulted in the highest cytotoxicity values among all other modalities (Fig 8). This confirms both the radiosensitization enhancement effects of HG and the synergetic cell killing actions of ST and the gold sensitized radiotherapy. The cytotoxicity of this model increases with increasing the molar concentration of both ST and HG.

Generally, it can be concluded that both the hydrophilic radiosensitizer (HG) and the hydrophobic chemotherapeutic (sorafenib tosylate) could be efficiently released from the hybrid nanoporous alginate/CaCO<sub>3</sub> and can be efficiently internalized into HepG2 cells resulting in significant and synergistic cytotoxic effects. Eventually, the gold-sensitized combinatorial model (HG-ST-ALG + radiation dose of 6 Gy) efficiently reduces the cell viability of HepG2 cells to less than 15%.

### Conclusions and future outlook

Nanoporous ALG-CaCO<sub>3</sub> hybrid matrix was prepared and utilized as a biocompatible platform for simultaneous encapsulation of the hydrophobic drug, sorafenib tosylate, and the hydrophilic radiosensitizer, hexagonal gold nanoparticles. A simple method was proposed for preparation of monodispersed stable nanoparticles featured with high payload and sustained drug release profile. *In-vitro* studies on HepG2 cells demonstrated that hexagonal gold nanoparticles can significantly enhance the radiobiological response of HepG2 cells to low doses of  $\gamma$ -radiation. Sorafenib-loaded alginate nanoparticles exhibited moderate cytotoxicity indicating the good release of ST from the nanoparticles. Treatment of HepG2 cells with the proposed combinatorial model (HG-ST-ALG + irradiation with 6 Gy) exhibited high toxicity and much higher than each individual treatment model. This evidences that the proposed design is significant in that it provides synergistic and combinatorial effects of two therapeutic modalities that are different

in their mechanisms of action. These promising *in-vitro* results suggest the prepared combinatorial model for further *in-vivo* studies.

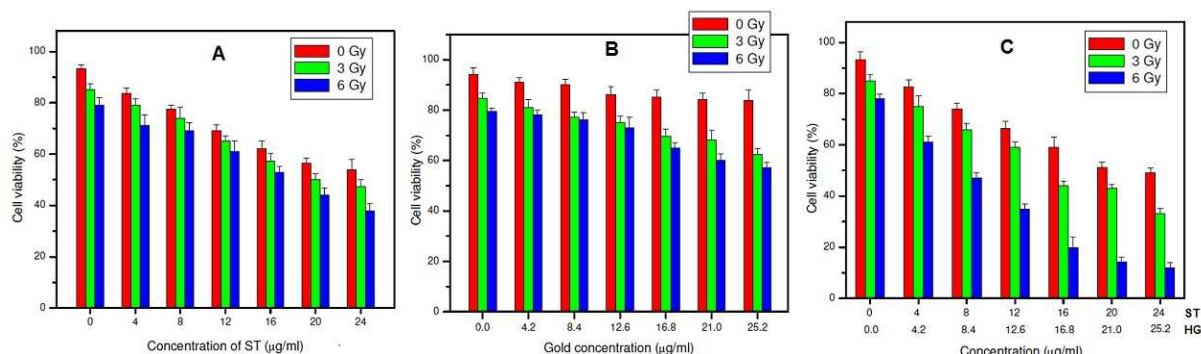


Fig. 8. Cell viability results obtained after treating HepG2 cell with the prepared formulations containing different concentrations of HG and ST followed by exposure to 0, 3 and 6 Gy.

### Declaration of interest

The authors report no conflict of interest.

### Acknowledgement

We are grateful for the financial support of (National Research Centre, Dokki, Giza, Egypt) within the In-house research project number 12020302.

### References

- [1] Ahmadi M., Madrakian T. and Ghavami S., Preparation and characterization of simvastatin nanocapsules, encapsulation of hydrophobic drugs in calcium alginate. *Methods Mol. Biol.*, 2125, 47-56(2020).
- [2] Markeb A., El-Maali N. and Sayed D., Synthesis, structural characterization, and preclinical efficacy of a novel paclitaxel-loaded alginate nanoparticle for breast cancer treatment. *Int. J Breast Cancer*, Article ID 7549372(2016).
- [3] Alipour S., Montaseri H., Khalili A. and Tafaghodi M., Non-invasive endotracheal delivery of paclitaxel-loaded alginate microparticles. *J. Chemother.*, 28, 411-416(2016).
- [4] Tokarev A., Agulhon P. and Long J., Synthesis and study of Prussian blue type nanoparticles in an alginate matrix. *J Mater. Chem.*, 22, 20232-20242(2012).
- [5] Puente P., Fettig N. and Luderer M., Injectable hydrogels for localized chemotherapy and radiotherapy in brain tumors. *J Pharm. Sci.*, 107, 922-933(2018).
- [6] Etienne T., A review on natural polymer derived injectable hydrogels for tissue engineering applications. *IJARW*, 1, 2582-1008(2020).
- [7] Ahmad A, Mubarak N., Jannat F., et al. A critical review on the synthesis of natural sodium alginate based composite materials: An innovative biological polymer for biomedical delivery applications. *Processes*, 9, 137-163(2021).
- [8] Zhang H., Cheng J. and Ao Q., Preparation of alginate-based biomaterials and their applications in biomedicine. *Mar. Drugs*, 19, 264-287(2021).
- [9] Swamy S., Kameshwar, V. and Shubha P., Targeting multiple oncogenic pathways for the treatment of hepatocellular carcinoma. *Target. Oncol.*, 12, 110-115(2016).
- [10] Gao J., Shi Z., Xia J. and Inagaki Y., Sorafenib-based combined molecule targeting in treatment of hepatocellular carcinoma. *World J Gastroenterol.*, 21, 12059-12070(2015).
- [11] Gana H., Chen, L. and Sui X., Enhanced delivery of sorafenib with anti-GPC3 antibody-conjugated TPGSb-PCL/Pluronic P123 polymeric nanoparticles for targeted therapy of hepatocellular carcinoma. *Mater. Sci. Eng. C*, 91, 395-403(2018).

- [12] Wang Y., Benzina A. and Molin D., Preparation and structure of drug-carrying biodegradable microspheres designed for transarterial chemoembolization therapy. *J Biomater. Sci., Polym. Ed*, 26, 77-91(2015).
- [13] Liu Te-I., Yang Y-C. and Chiang W-H., Radiotherapy-controllable chemotherapy from ROS-responsive polymeric nanoparticles for effective local dual modality treatment of malignant tumors. *Biomacromolecules*, 19, 3825-3839(2018).
- [14] Liu C., Wang C. and Chien C. Enhanced X-ray irradiation-induced cancer cell damage by gold nanoparticles treated by a new synthesis method of polyethylene glycol modification. *Nanotechnology*, 19, 295104(2008).
- [15] Kwatral D., Venugopal A. and Anant S., Nanoparticles in radiation therapy, a summary of various approaches to enhance radiosensitization in cancer. *Transl. Cancer Res.*, 2, 330-342(2013).
- [16] Kobayashi K., Usami N. and Porcel E., Enhancement of radiation effect by heavy elements. *Mutat. Res.*, 704, 123-131(2010).
- [17] Liu X., Liu Y. and Zhang P., The synergistic radiosensitizing effect of tirapazamine-conjugated gold nanoparticles on human hepatoma HepG2 cells under X-ray irradiation. *Int. J Nanomed.* 11, 3517-3531(2016).
- [18] Ma N., Wu F-G. and Zhang X., Shape-dependent radiosensitization effect of gold nanostructures in cancer radiotherapy, Comparison of gold nanoparticles., nanospikes., and nanorods. *ACS Appl. Mater. Interfaces*, 9, 13037-13048(2017).
- [19] Butterworth K., McMahon S., Currellab F. and Prise K., Physical basis and biological mechanisms of gold nanoparticle radiosensitization. *Nanoscale*, 4, 4830-4838(2012).
- [20] Hainfeld J., Slatkin D. and Smilowitz H., The use of gold nanoparticles to enhance radiotherapy in mice. *Phys. Med. Biol.*, 49, N309-N315(2004).
- [21] Yoon J., Cho H., Hyo-Eon H. and Maeng H., Mitoxantrone-loaded PEGylated gold nanocomplexes for cancer therapy. *J Nanosci. Nanotechnol.*, 19, 687-690(2019).
- [22] Shanei A. and Sazgarnia A., Dual function of gold nanoparticles in synergism with mitoxantrone and microwave hyperthermia against melanoma cells. *Asian Pac. J Cancer Prev.*, 18, 2911-2917(2017).
- [23] Alkhatib M., Alnahdi N. and Backer W., Antitumor activity., hematotoxicity and hepatotoxicity of sorafenib formulated in a nanoemulsion based on the carrot seed oil. *Int. J Life Sci. Pharma. Res.*, 8, 50-57(2018).
- [24] Yong H., Xiqun J. and Yin D., Synthesis and characterization of chitosan-poly(acrylic acid) nanoparticles. *Biomaterials*, 23, 3193-3201(2002).
- [25] Sondermeije H., Witkowski P. and Woodland D., Optimization of alginate purification using polyvinylidene difluoride membrane filtration, Effects on immunogenicity and biocompatibility of three-dimensional alginate scaffolds. *Biomater. Appl.*, 3, 510-520(2016).
- [26] Bondi M., Angela A. and Giuseppe Sortino G., Nanoassemblies based on supramolecular complexes of nonionic amphiphilic cyclodextrin and sorafenib as effective weapons to kill human HCC cells. *Biomacromolecules*, 16, 3784-3791(2015).
- [27] Wanga Y., Benzinaa A. and Molin D., Preparation and structure of drug-carrying biodegradable microspheres designed for transarterial chemoembolization therapy. *J Biomater. Sci., Polym. Ed*, 26, 77-91(2015).
- [28] Talaat R., Abo-Zeid T. and Abo-Elfadl M., Combined hyperthermia and radiation therapy for treatment of hepatocellular carcinoma. *Asian Pac. J Cancer Prev.*, 20, 2303-2310.
- [29] Hamzian N., Hashemi M. and Gorbani M., In-vitro study of multifunctional plga-spion nanoparticles loaded with gemcitabine as radiosensitizer used in radiotherapy. *Iran. J Pharm. Res.*, 18, 1694-1703(2019).
- [30] Hu J., Wang Z. and Li J., Gold nanoparticles with special shapes, controlled synthesis., surface-

enhanced raman scattering., and the application in biodetection. *Sensors*,7, 3299-3311(2007).

[31] Kuo C-H., Chiang T-F. and Chen L-J., Synthesis of highly faceted pentagonal- and hexagonal-shaped gold nanoparticles with controlled sizes by sodium dodecyl sulfate. *Langmuir*, 20, 7820-7824(2004).

[32] Peng P., Meng A. and Braun M., Plasmons and inter-band transitions of hexagonal close packed gold nanoparticles. *Appl. Phys. Lett.*, 115, 051107(2019).

[33] Wei W., Ma G., Hu G., et al. Preparation of hierarchical hollow CaCO<sub>3</sub> particles and the application as anticancer drug carrier. *Am. Chem. Soc.*, 130, 15808-15810(2008).

[34] Peng C., Zhao Q. and Gao C., Sustained delivery of doxorubicin by porous CaCO<sub>3</sub> and chitosan/alginate multilayers-coated CaCO<sub>3</sub> microparticles. *Colloids Surf. A, Physicochem.Eng. Aspects*, 353, 132(2010).

[35] Wu J-L., Wang C-Q. and Zhuo R-X., Multi-drug delivery system based on alginate/calcium carbonate hybrid nanoparticles for combination chemotherapy. *Colloids Surf. B Biointerfaces*,123, 498-505(2014).

[36] Jeevana B, and Keerthi M., *Int. J Pharm. Sci. Rev.*, 67, 210-216(2021).

[37] Chountoules M., Naziris N., Mavromoustakos T. and Demetzos C., *Methods Mol. Biol.*, 2207, 299-305(2021).

[38] Abulateefeh S. and Taha M., *J Microencapsul.*,32, 96-102(2015).

[39] Ibrahim H., Farid O. and Samir A., Preparation of chitosan antioxidant nanoparticles as drug delivery system for enhancing of anti-cancer drug. *Key Eng. Mater.*, 759, 92-97(2018).

[40] Prabakaran M., Chitosan-based nanoparticles for tumor-targeted drug delivery. *Int.J Biol. Macromol.*,72, 1313-1322(2015).

[41] Yu X., Hou J. and Shi Y., Preparation and characterization of novel chitosan-protamine nanoparticles for nucleus-targeted anticancer drug delivery. *Int. J Nanomed.*, 11, 6035-6046(2016).

[42] Vishwakarma S., Sharmila P. and Bardia A., *Sci. Rep.*, 7, 8539-8544(2017).

[43] Parveen S. and Sahoo S., Long circulating chitosan/PEG blended PLGA nanoparticle for tumor drug delivery. *Eur. J pharmacol.*, 670, 372-383(2011).

#### الملخص العربي

في هذا البحث تمت دراسة التأثيرات السمية الخلوية الإندماجية لعقار السورافينيب توزيلات بالتزامن مع إشعاع جاما على خلايا سرطان الكبد. تم تحضير جزيئات الذهب النانوية ذات الشكل الهندسي السداسي وقد أثبتت هذه الجزيئات النانوية كفاءة عالية في رفع إستجابة خلايا سرطان الكبد لجرعات صغيرة أو متوسطة من إشعاع جاما العلاجي. تم أيضا دمج جزيئات الذهب النانوية مع العقار الكيماوي المضاد لسرطان الكبد (السورافينيب توزيلات) في كبسولات نانوية حيوية معتمدة على المترابك البوليمري الحيوي غير المتجانس (ألجينات الصوديوم-كربونات الصوديوم) لتحقيق تجانس حيوي وتحقيق تأثير متزامن وغير متعارض لنوعى العلاج (الكيماوي والإشعاعي المحفز بجزيئات الذهب النانوية). ساعد التركيب غير المتجانس ذو المسام النانوية على امكانية استضافة العقار الكاره للماء (السورافينيب توزيلات) في حين ساعدت المواقع المحبة للماء في البوليمر الحيوي (ألجينات) على إحتواء المحفز الإشعاعي (جزيئات الذهب السداسية النانوية). أثبتت الدراسة على خلايا سرطان الكبد من النوع (HepG2) كفاءة عالية ومتزامنة في قتل خلايا السرطان وهي كفاءة أعلى من الكفاءة الناتجة من إستخدام أى من العلاجات بصورة منفردة. النتائج تشير الى أن التركيبات المحضرة واعدة جدا كعلاج (كيماوي- إشعاعي) مزدوج لقتل خلايا سرطان الكبد باستخدام جرعات أقل من الإشعاع وأثار جانبية أقل.